

## Dzhuluite, $\text{Ca}_3\text{SbSnFe}^{3+}_3\text{O}_{12}$ , a new bitikleite-group garnet from the Upper Chegem Caldera, Northern Caucasus, Kabardino-Balkaria, Russia

IRINA O. GALUSKINA<sup>1,\*</sup>, EVGENY V. GALUSKIN<sup>1</sup>, JOACHIM KUSZ<sup>2</sup>, PIOTR DZIERŻANOWSKI<sup>3</sup>, KRYSZTIAN PRUSIK<sup>4</sup>,  
VIKTOR M. GAZEEV<sup>5</sup>, NIKOLAI N. PERTSEV<sup>5</sup> and LEONID DUBROVINSKY<sup>6</sup>

<sup>1</sup> Faculty of Earth Sciences, Department of Geochemistry, Mineralogy and Petrography, University of Silesia, Będzińska 60, 41–200 Sosnowiec, Poland

\*Corresponding author, e-mail: irina.galuskina@us.edu.pl

<sup>2</sup> Institute of Physics, University of Silesia, Uniwersytecka 4, 40–007 Katowice, Poland

<sup>3</sup> Institute of Geochemistry, Mineralogy and Petrology, Warsaw University, al. Żwirki i Wigury 93, 02–089 Warszawa, Poland

<sup>4</sup> Institute of Materials Science, University of Silesia, 75 Pułku Piechoty 1A 12, 41–500 Chorzów, Poland

<sup>5</sup> Institute of Geology of Ore Deposits, Geochemistry, Mineralogy and Petrography (IGEM) RAS, Staromonetny 35, Moscow, Russia

<sup>6</sup> Bayerisches Geoinstitut, Universität Bayreuth, 95440 Bayreuth, Germany

**Abstract:** Dzhuluite,  $\text{Ca}_3\text{SbSnFe}^{3+}_3\text{O}_{12}$  ( $Ia\bar{3}d$ ,  $a = 12.536(3)$  Å,  $V = 1970.05(9)$  Å<sup>3</sup>,  $Z = 8$ ), a new antimony garnet of the bitikleite-group, was discovered in a kumtyubeite zone in close proximity to the contact with unaltered ignimbrite in a skarn xenolith from the Upper Chegem Caldera, Northern Caucasus, Russia. The empirical formula of the holotype dzhuluite is  $(\text{Ca}_{2.954}\text{Fe}^{2+}_{0.043}\text{Mg}_{0.003})_{\Sigma 3.000} (\text{Sn}_{0.850}\text{Sb}^{5+}_{0.764}\text{Zr}_{0.121}\text{U}^{6+}_{0.127}\text{Ti}^{4+}_{0.070}\text{Sc}_{0.009}\text{Nb}^{5+}_{0.058}\text{Hf}_{0.001})_{\Sigma 2.001} (\text{Fe}^{3+}_{2.051}\text{Al}_{0.653}\text{Fe}^{2+}_{0.182}\text{Ti}^{4+}_{0.087}\text{Si}_{0.028})_{\Sigma 3.001}\text{O}_{12}$ . Associated minerals are kumtyubeite, cuspidine, fluorchegemite, larnite, fluorite, wadalite, rondorfite, hydroxyllestadite, perovskite, lakargiite, kerimasite, elbrusite, srebrodolskite, bultfonteinite, ettringite group minerals, hillebrandite, afwillite, tobermorite-like minerals, hydrocalumite and hydrogrossular. Dzhuluite forms poikilitic crystals < 50 μm in size that are light-yellow to dark-brown and with a creamy streak. The lustre is strongly vitreous. The calculated density of dzhuluite ranges from 4.708 to 4.750 g/cm<sup>3</sup>. Raman spectra are analogous to those of kimzeyite, kerimasite and other bitikleite-group minerals. Dzhuluite formed at high temperature during a retrograde stage of primary rock alteration in the larnite subfacies (sanidinite facies) as a result of fluorine metasomatism.

**Key-words:** dzhuluite, new mineral, garnet, bitikleite-group, solid solution, Raman spectroscopy, EBSD, Upper Chegem Caldera, skarn.

### Introduction

Dzhuluite, a new antimony garnet with the end-member formula  $\text{Ca}_3\text{SbSnFe}^{3+}_3\text{O}_{12}$ , was discovered in an altered carbonate-silicate xenolith in ignimbrites of the Upper Chegem caldera, Northern Caucasus, Kabardino-Balkaria, Russia. Dzhuluite was approved by the IMA Commission on New Minerals, Nomenclature and Classification (CNMNC) under the name “bitikleite-(SnFe)”, IMA2010-064 (Galuskina *et al.*, 2011a). However, in 2011, a subcommittee elaborating a new classification of the garnet supergroup, on which two of the authors of this paper (I. G. and E. G.) served, recommended not to use Levinson suffixes in naming minerals of the garnet supergroup except for menzerite-(Y) (Grew

*et al.*, 2013). In line with the recommendation, the garnet subcommittee renamed four minerals of the garnet supergroup and the IMA CNMNC approved these changes. The name changes relate to minerals of the bitikleite-group discovered recently in skarn xenoliths of the Upper Chegem Caldera. The name bitikleite-(SnAl) was changed to bitikleite; bitikleite-(ZrFe) to usturite (after Ustur Mountain in the field-work area); bitikleite-(SnFe) to dzhuluite (after Dzhulu Mountain nearby near the field-work area) and elbrusite-(Zr) to elbrusite (Grew *et al.*, 2013). In addition, the new end-member formula of elbrusite,  $\text{Ca}_3(\text{U}^{6+}_{0.5}\text{Zr}_{1.5})\text{Fe}^{3+}_3\text{O}_{12}$ , was accepted by the subcommittee (Grew *et al.*, 2013). The first description of bitikleite and usturite using the old names bitikleite-(SnAl) and bitikleite-(ZrFe), respectively, were published

earlier (Galuskina *et al.*, 2010 a). The name bitikleite-(SnFe) was used only once in Newsletter 8 of the IMA CNMNC (Williams *et al.*, 2011). The old names of these minerals should now be replaced by their new names in all mineralogical databases.

Altered under sanidinite-facies conditions, carbonate-silicate xenoliths of sedimentary rocks in ignimbrites of the Upper Chegem Caldera are mineralogically unique; more than 20 new minerals have been discovered in them over the five last years. Interestingly, minerals of the garnet supergroup and of the humite group prevail among these new mineral species. Minerals of the garnet supergroup are represented by bitikleite  $\text{Ca}_3(\text{Sb}^{5+}\text{Sn})\text{Al}_3\text{O}_{12}$ , usturite  $\text{Ca}_3(\text{Sb}^{5+}\text{Zr})\text{Fe}^{3+}_3\text{O}_{12}$ , dzhuluite  $\text{Ca}_3(\text{Sb}^{5+}\text{Sn})\text{Fe}^{3+}_3\text{O}_{12}$ , elbrusite  $\text{Ca}_3(\text{U}^{6+}_{0.5}\text{Zr}_{1.5})\text{Fe}^{3+}_3\text{O}_{12}$ , toturite  $\text{Ca}_3\text{Sn}_2\text{Fe}_2\text{SiO}_{12}$  and irinarassite  $\text{Ca}_3\text{Sn}_2\text{Fe}_2\text{AlO}_{12}$  (Galuskina *et al.*, 2010a–c; Galuskina *et al.*, 2011b). Minerals of the humite group are represented by the Cahumite minerals: kumtyubeite  $\text{Ca}_5(\text{SiO}_4)_2\text{F}_2$  (Galuskina *et al.*, 2009), chegemite  $\text{Ca}_7(\text{SiO}_4)_3(\text{OH})_2$  (Galuskina *et al.*, 2009), fluorchegemite  $\text{Ca}_7(\text{SiO}_4)_3\text{F}_2$  (Galuskina *et al.*, 2012), edgrewite  $\text{Ca}_9(\text{SiO}_4)_4\text{F}_2$  and hydroxyledgrewite  $\text{Ca}_9(\text{SiO}_4)_4(\text{OH})_2$  (Galuskina *et al.*, 2012).

Dzhuluite  $\text{Ca}_3(\text{Sb}^{5+}\text{Sn})\text{Fe}^{3+}_3\text{O}_{12}$  is the  $\text{Fe}^{3+}$ -analogue of bitikleite  $\text{Ca}_3(\text{Sb}^{5+}\text{Sn})\text{Al}_3\text{O}_{12}$ , both of which were discovered in the same xenolith (Galuskina *et al.*, 2011a). The synthetic analogue of dzhuluite  $\text{Ca}_3\text{SbSnFe}_3\text{O}_{12}$  ( $a = 12.634 \text{ \AA}$ ) was synthesized about forty years ago (Dodokin *et al.*, 1972). A typical dzhuluite sample, under the name bitikleite-(SnFe) and with the number 4025/1, is deposited in the collection of the Fersman Mineralogical Museum in Moscow, Russia.

## Analytical methods

The morphology and composition of the Sb-garnet crystals were investigated using a Philips/FEI ESEM XL30/EDAX scanning electron microscope and a CAMECA SX100 electron-microprobe analyzer. Electron-microprobe analyses (EPMA) of the garnets were performed at 15 kV and 40–50 nA using the following lines and standards:  $\text{MgK}\alpha$  - diopside,  $\text{AlK}\alpha$  - orthoclase,  $\text{SiK}\alpha$ ,  $\text{CaK}\alpha$  - wollastonite,  $\text{ScK}\alpha$  - Sc,  $\text{TiK}\alpha$  - rutile,  $\text{VK}\alpha$  -  $\text{V}_2\text{O}_5$ ,  $\text{CrK}\alpha$  -  $\text{Cr}_2\text{O}_3$ ,  $\text{MnK}\alpha$  - rhodonite,  $\text{FeK}\alpha$  - hematite,  $\text{SrL}\alpha$  -  $\text{SrTiO}_3$ ,  $\text{YL}\alpha$  - YAG,  $\text{ZrL}\alpha$  - zircon,  $\text{NbL}\alpha$  - Nb,  $\text{SnL}\alpha$  - cassiterite,  $\text{SbL}\alpha$  - InSb,  $\text{HfM}\alpha$  - Hf,  $\text{ThM}\alpha$  -  $\text{ThO}_2$ ,  $\text{UM}\beta$  - syn. $\text{UO}_2$  and vorlanite  $\text{CaUO}_4$ .

Single-crystal X-ray studies were carried out using an Xcalibur/CCD diffractometer ( $\text{MoK}\alpha$ ,  $\lambda = 0.71073 \text{ \AA}$ ). However, because of the small crystal size of the dzhuluite and its marked inhomogeneity, only unit-cell parameters were determined.

Because of the small size of the dzhuluite crystals, electron backscatter diffraction (EBSD) analysis was used for structural-parameters and symmetry determination. The EBSD images were recorded with a HKL Nordlys II camera attached to a JSM-6480 scanning

electron microscope using 30 kV beam energy. The microprobe thin section on which composition measurements were performed was re-polished using an  $\text{Al}_2\text{O}_3$  suspension of 20 nm particle size. Calibration of SEM and EBSD geometry was carried out using a single Si crystal for two detector distances: 177 mm (normal working position) and 150 mm (camera retracted position). The program “Chanel5” (Oxford Instruments) was used for the interpretation of the EBSD diffraction patterns. Structural data were obtained using EBSD and fitting data according to modeling on the basis of bitikleite ( $a = 12.5240(2) \text{ \AA}$ ) and usturite ( $a = 12.491 \text{ \AA}$ ) structures (Galuskina *et al.*, 2010a). The cell constant of the dzhuluite was calculated using the formula of Strocka *et al.* (1978),  $a = b_1 + b_2r_X + b_3r_Y + b_5r_Xr_Y + b_6r_Xr_Z + b_4r_Z$  ( $\text{\AA}$ ), where  $b_1 = 7.02954$ ,  $b_2 = 3.31277$ ,  $b_3 = 2.49398$ ,  $b_4 = 3.34124$ ,  $b_5 = -0.87758$ ,  $b_6 = -1.38777$ , and  $r_X$ ,  $r_Y$ ,  $r_Z$  are weighted averages of effective ionic radii of cations in the X, Y and Z sites, respectively (Shannon, 1976).

Raman spectra of single dzhuluite crystals were recorded using a Dilor XY spectrophotometer (Bayerisches Geoinstitut, University of Bayreuth, Germany) equipped with a 1800 line  $\text{mm}^{-1}$  grating monochromator, a charge-coupled device, a Peltier-cooled detector and an Olympus BX40 confocal microscope. The incident laser excitation was provided by a water-cooled argon laser source operating at 514.5 nm. The power at the exit of a 100 $\times$  objective lens varied from 30 to 50 mW. Raman spectra were recorded in backscattering geometry in the range 100–4000  $\text{cm}^{-1}$  and with a resolution of 2  $\text{cm}^{-1}$ . Collection times of 20 s and accumulations of 5 scans were chosen. The monochromator was calibrated using the Raman scattering line of a silicon plate (520.7  $\text{cm}^{-1}$ ).

## Occurrence

The dzhuluite was found in a kumtyubeite zone, 0.2–0.5 m in thickness, at the northern end of xenolith No. 1 in close proximity to the contact with unaltered ignimbrite (see geological scheme in Galuskina *et al.*, 2009). Xenolith No. 1, about 20 m in longest dimension, is the largest xenolith among those known in the ignimbrites of the Upper Chegem Caldera. The xenoliths are characterized by high-temperature mineral associations of the sanidinite facies typical of pyrometamorphic rocks: larnite, spurrite, galuskinite, rondorfite, fluor- and hydroxylellestadite, srebrodolomite, magnesioferrite. Galuskinite,  $\text{Ca}_7(\text{SiO}_4)_3\text{CO}_3$ , is a new mineral discovered recently in skarns of the Birkhin Massif, Baikal, Russia (Lazic *et al.*, 2011). A full description of the geology of this area, and of the skarn zonation of the xenolith No. 1, may be found in Gazeev *et al.* (2006) and Galuskina *et al.* (2008, 2009).

Dzhuluite was detected in an altered inhomogeneous kumtyubeite zone with abundant ettringite-taumasite, katoite-hydrogrossular, bultfonteinite, hillebrandite, awfillite, jennite and other unidentified calcium hydrosilicates (Fig. S1 in Supplementary material, freely available

online at the GSW website of the journal: <http://eurjmin.geoscienceworld.org/>). Primary high-temperature minerals are represented by larnite relics, spurrite, wadalite, As-bearing hydroxyllestadite, rondorfite and accessory lakargiite, perovskite and magnesioferrite.

The kumtyubeite (Kmt) rocks, and the local development of fluorchegemite and cuspidine in them, reflect the retrograde alteration of primary high-temperature rocks by fluorine metasomatism of rocks fragments enriched in spurrite (Spu) according to the reaction  $\text{Ca}_5(\text{SiO}_4)_2\text{CO}_3$  (Spu) +  $2\text{HF} = \text{Ca}_5(\text{SiO}_4)_2\text{F}_2$  (Kmt) +  $\text{CO}_2 + \text{H}_2\text{O}$ . Larnite (Lar) was replaced by cuspidine (Cus) according to the reaction  $\text{Ca}_2\text{SiO}_4$  (Lar) +  $2\text{HF} = \text{Ca}_4(\text{Si}_2\text{O}_7)\text{F}_2$  (Cus) +  $\text{H}_2\text{O}$  and, presumably, fluorchegemite (Fch) formed after galuskinite (Gal) by the reaction  $\text{Ca}_7(\text{SiO}_4)_3\text{CO}_3$  (Gal) +  $2\text{HF} = \text{Ca}_7(\text{SiO}_4)_3\text{F}_2$  (Fch) +  $\text{CO}_2 + \text{H}_2\text{O}$ . Commonly, the formation of fluorine silicates was accompanied by fluorite crystallization. The high-fluorine environment influenced the formation of garnets with exotic composition. Simultaneous growth of cuspidine and bitikleite crystals is observed (see Fig. 1d in Galuskina *et al.*, 2010a).

Dzhuluite occurs as {211} crystals not exceeding 15  $\mu\text{m}$  in size with cores of the analogue of kerimasite with  $\text{Ti} > \text{Si}$  at tetrahedral site (Table 1, analyses 3, 4; Fig. 1a). Dzhuluite also forms later zones on granular pseudomorphs of

lakargiite after zircon (Fig. 1b). Less commonly, xenomorphic poikilitic crystals of dzhuluite are crowded by inclusions of wadalite crystals or katoite-grossular pseudomorphs after wadalite, in some cases substituted by cuspidine (Fig. 1c, d). The size of poikilitic dzhuluite crystals is typically less than 20  $\mu\text{m}$  (Fig. 1c; Table 1, analyses 5, 6) though some may reach 50  $\mu\text{m}$  (Fig. 1d; Table 1, analysis 7). The dzhuluite crystals are commonly inhomogeneous in composition and display weak core-to-rim trends of increasing contents of U, Nb and Sn; they belong to a complex solid-solution series in which the  $\text{Ca}_3\text{SnSbFe}_3\text{O}_{12}$  end-member content reaches up to 68.5 mol% (Table 1). U, Zr, Ti, Al, Nb are the main impurities. The  $\text{SiO}_2$  content does not exceed 0.5 wt% (Table 1). Some dzhuluite crystals are overgrown by elbrusite (Fig. S2). Rare poikilitic crystals with the elbrusite end-member prevailing were noted (Table 1, analysis 8). High U contents are not characteristic of the other Sb-garnets, bitikleite and usturite, known in the skarn xenoliths of the Upper Chegem Caldera, whereas U is commonly the main impurity in kerimasite  $\text{Ca}_3\text{Zr}_2\text{Fe}^{3+}_2\text{SiO}_{12}$ , forming a continuous isomorphic series with elbrusite (Galuskina *et al.*, 2010 a–c).

The dzhuluite crystals are light-yellow to dark-brown with a creamy streak. The lustre is strongly vitreous. The new garnet is optically isotropic ( $n = 1.94$ , based on a

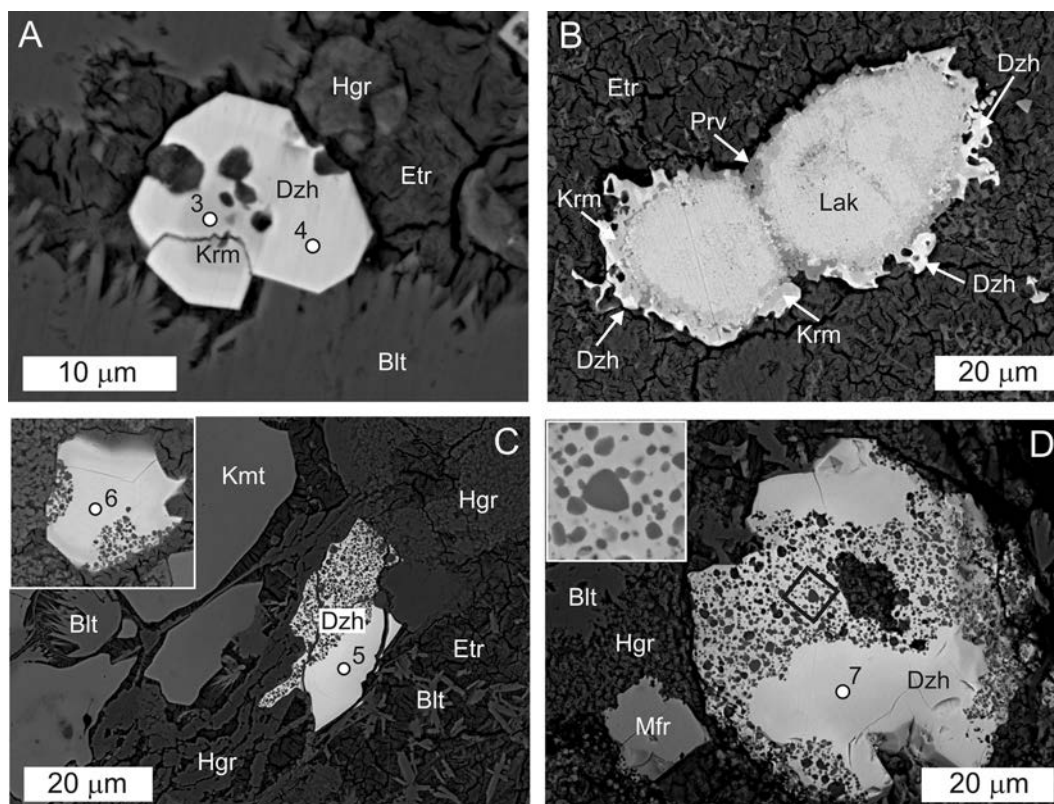


Fig. 1. A – dzhuluite crystal with kerimasite core; B – inhomogeneous pseudomorph of lakargiite after zircon with external rim composed by kerimasite, dzhuluite and perovskite; C – xenomorphic poikilitic crystals of dzhuluite used for Raman spectroscopy analyses and (inset) crystal used for EBSD study. Scale refers to both crystals; D – the largest poikilitic crystal of dzhuluite with trioctahedral wadalite inclusions and (inset) magnified fragment. Blt bullfontinite, Dzh – dzhuluite, Mfr – magnesioferrite, Krm – kerimasite, Hgr – grossular-katoite, Etr – ettringite, Prv – perovskite. Numbers identify points where EPMA, Raman and EBSD analyses were performed (see text).

Table 1. Chemical composition of dzhuluite (Dzh), kerimasite (Krm) and elbrusite (Elb) from the kumtyubeite zone of altered xenolith from the Upper Chegem Caldera.

	1		2		3		4		5		6		7		8	
	Dzh		Dzh		Krm		Dzh		Dzh		Dzh		Dzh		Elb	
	mean 9	SD	range	mean 9	SD	range	Fig. 1A	Fig. 1B	Fig. 1C	Fig. 1D	Fig. 1E	Fig. 1F	Fig. 1G	Fig. 1H	Fig. 1I	Fig. 1J
UO <sub>3</sub> (wt.%)	6.30	1.06	4.78–8.40	5.19	1.28	3–6.84	0.70	8.40	4.61	4.30	11.28	20.37				
V <sub>2</sub> O <sub>5</sub>	n.d.	n.d.					n.d.	n.d.	0.07	n.d.	n.d.	n.d.				
Nb <sub>2</sub> O <sub>5</sub>	0.08	0.06	0–0.17	1.10	0.21	0.76–1.44	n.d.	n.d.	1.01	1.08	0.70	1.17				
Sb <sub>2</sub> O <sub>5</sub>	16.73	1.84	14.24–19.43	17.67	1.33	16.14–19.32	9.51	16.81	19.22	19.32	14.50	8.68				
SiO <sub>2</sub>	0.28	0.09	0.17–0.42	0.24	0.06	0.14–0.30	1.75	0.23	0.15	0.18	0.11	0.28				
TiO <sub>2</sub>	2.62	0.35	2.13–3.05	1.79	0.50	1.03–2.73	5.39	2.13	1.45	1.56	0.72	1.56				
ZrO <sub>2</sub>	4.21	1.34	2.78–6.20	2.13	2.01	0–5.07	20.64	3.37	n.d.	0.75	0.08	6.35				
SnO <sub>2</sub>	16.70	0.64	15.64–17.44	18.32	1.82	15.59–20.82	9.74	16.78	20.57	19.47	21.27	7.18				
HfO <sub>2</sub>	n.d.			n.d.			0.46	n.d.	n.d.	n.d.	n.d.	n.d.				
Al <sub>2</sub> O <sub>3</sub>	6.17	0.38	5.20–6.46	4.76	0.23	4.47–5.14	6.23	5.20	5.14	5.12	4.52	2.93				
Se <sub>2</sub> O <sub>3</sub>	0.05	0.05	0–0.15	0.09	0.09	0–0.21	n.d.	n.d.	0.12	0.05	0.14	0.08				
Fe <sub>2</sub> O <sub>3</sub> *	19.82	0.55	18.93–20.46	23.47	0.63	22.45–24.43	19.22	19.92	23.01	23.51	20.82	23.52				
FeO*	2.20	0.41	1.75–3.21	2.27	0.36	1.92–3.17	0.09	3.13	2.19	2.32	3.79	3.59				
MgO	0.02	0.02	0–0.05	0.02	0.01	0.00–0.04	n.d.	0.03	0.03	0.02	0.03	0.08				
CaO	23.86	0.24	23.53–24.17	23.70	0.29	23.2–24.04	25.49	23.60	24.04	23.85	22.84	22.92				
MnO	n.d.			n.d.			n.d.	n.d.	n.d.	n.d.	n.d.	0.09				
Total	99.04			100.74			99.22	99.60	101.61	101.52	100.80	98.80				
Ca	2.999			2.955			3.003	3.008	2.979	2.948	2.964	3.050				
Mn												0.009				
Mg	0.001			0.003					0.005	0.003	0.005					
Fe <sup>2+</sup>				0.042					0.016	0.049	0.031					
X	<b>3.000</b>			<b>3.000</b>			<b>3.003</b>	<b>3.008</b>	<b>3.000</b>	<b>3.000</b>	<b>3.000</b>	<b>3.059</b>				
Sn <sup>4+</sup>	0.781			0.850			0.427	0.796	0.949	0.896	1.002	0.355				
Sb <sup>5+</sup>	0.729			0.764			0.388	0.743	0.826	0.828	0.652	0.400				
U <sup>6+</sup>	0.155			0.127			0.016	0.210	0.112	0.104	0.287	0.531				
Zr	0.241			0.121			1.107	0.196	0.000	0.042	0.005	0.385				
Ti <sup>4+</sup>	0.082			0.072			0.044	0.042	0.048	0.067	0.042	0.146				
Nb <sup>5+</sup>	0.004			0.058					0.053	0.056	0.038	0.066				
Hf							0.014									
Sc	0.005			0.009					0.012	0.005	0.015	0.009				
Mg	0.002							0.005				0.015				
Fe <sup>2+</sup>												0.034				
Y	<b>1.999</b>			<b>2.000</b>			<b>1.997</b>	<b>1.992</b>	<b>1.999</b>	<b>2.000</b>	<b>1.999</b>	<b>1.941</b>				
Fe <sup>3+</sup>	1.749			2.055			1.590	1.783	2.003	2.041	1.898	2.198				
Al	0.853			0.653			0.807	0.729	0.701	0.696	0.645	0.429				
Ti <sup>4+</sup>	0.149			0.085			0.402	0.149	0.078	0.068	0.066	0.035				
Si <sup>4+</sup>	0.033			0.028			0.192	0.027	0.017	0.021	0.013	0.339				
Fe <sup>2+</sup>	0.216			0.179			0.008	0.311	0.196	0.174	0.353	0.339				
V <sup>5+</sup>									0.005							
Sn <sup>4+</sup>												0.025				
Z	<b>3.000</b>			<b>3.000</b>			<b>3.000</b>	<b>3.000</b>	<b>3.000</b>	<b>3.000</b>	<b>3.000</b>	<b>3.000</b>				



Table 1. continued.

1	2		3		4		5		6		7		8	
	Dzh	SD	mean	range	Krm	Dzh	Dzh	Dzh	Dzh	Dzh	Dzh	Dzh	Dzh	Elb
	mean	9	83%		Fig. 1A	73%	86%	86%	86%	86%	80%	80%	84%	
	SD		11%			17%	9%	9%	9%	9%	8%	8%	4%	
			6%			10%	5%	5%	5%	5%	12%	12%	11%	
			8.966			8.862	8.909	8.915	8.915	8.915	8.751	8.751	8.699	
			58%			59.4%	66.8%	68%	68%	68%	63.3%	63.3%	35.5%	
			<b>0.09</b>			<b>0.12</b>	<b>0.06</b>	<b>0.06</b>	<b>0.06</b>	<b>0.06</b>	<b>0.16</b>	<b>0.16</b>	<b>0.30</b>	

\*dpa – displacement per atom

Gladstone-Dale calculation of analysis 1, Table 1). The calculated density is 4.708 g/cm<sup>3</sup> based on analysis 1 (Table 1) and 4.750 g/cm<sup>3</sup> based on analysis 2 (Table 1).

## Crystallography

The marked inhomogeneity of the dzhuluite crystals, the abundance of wadalite and hydrogarnet inclusions, and also their small size and partial metamictization, did not permit obtaining full structural data. The single-crystal X-ray study of the U-bearing kimzeyite [UO<sub>3</sub> ≈ 10 wt%, cumulative dose dpa (displacement per atom) = 0.12] showed that it has a partially metamict structure and that uranium is concentrated in metamict domains (Galuskina *et al.*, 2010a). The calculated dpa fluctuates from 0.06 to 0.12 for dzhuluite (Table 1). Investigation of the kerimaite-elbrusite series showed that the critical dose for metamictization of these garnet is at dpa = 0.25–0.30 (Galuskina *et al.*, 2010a).

Only unit-cell parameters,  $Ia\bar{3}d$ ,  $a = 12.536(3)$  Å,  $V = 1970.05(9)$  Å<sup>3</sup>,  $Z = 8$ , were obtained for the 15 μm {211} dzhuluite crystal, the composition of which is close to analysis 4 in Table 1 (dpa = 0.1). This crystal has skeletal overgrowths of elbrusite 1–2 μm in thickness (Fig. S3), as revealed by the single-crystal X-ray diffraction study.

The EBSD patterns for the dzhuluite were obtained at working distances of 150 mm and 177 mm. Fitting of the EBSD data (WD 150 mm) of the crystals shown in Fig. 1A (calculated  $a = 12.56$  Å) and in Fig. 1d (calculated  $a = 12.60$  Å) to a garnet model with  $a = 12.55$  Å resulted in excellent fitting parameters MAD = 0.23° and 0.16°, respectively (Fig. 2).

Due to the scarcity of dzhuluite, and the small size of available crystals, powder X-ray diffraction data for the natural material were not collected, but data for analysis 1 (Table 1) with  $a = 12.55$  Å were calculated and are listed in Table S1.

## Raman spectroscopy

Raman spectra of dzhuluite (Fig. 3) are similar to those of other minerals of the bitikleite group and to Zr-bearing garnets of the schorlomite group (Galuskina *et al.*, 2011a). These spectra are characterized by the low intensities and broadening of bands in the 850–650 cm<sup>-1</sup> range defined by symmetric stretching vibrations in tetrahedron [ZO<sub>4</sub>] due to the fact that the tetrahedral site can be occupied by different cations (Fe, Ti, Al, *etc.*). The broad band between 850–650 cm<sup>-1</sup> which is centred at about 750–770 cm<sup>-1</sup> is mainly connected with vibrations in [Fe<sup>3+</sup>O<sub>4</sub>]<sup>5-</sup> which are seen at 730–750 cm<sup>-1</sup>, and also with vibrations in [AlO<sub>4</sub>]<sup>5-</sup> observed at the 800–780 cm<sup>-1</sup>. The broadening of this band reflects vibrations in [TiO<sub>4</sub>]<sup>4-</sup>, bands from which can fall between bands from [Fe<sup>3+</sup>O<sub>4</sub>]<sup>5-</sup> and [AlO<sub>4</sub>]<sup>5-</sup> vibrations on the Raman spectrum. Most probably, the broadening of the band is accounted for by overlapping of vibrations in [Fe<sup>2+</sup>O<sub>4</sub>]<sup>6-</sup>, the frequency of which is below the frequency of vibrations in [Fe<sup>3+</sup>O<sub>4</sub>]<sup>5-</sup>. The

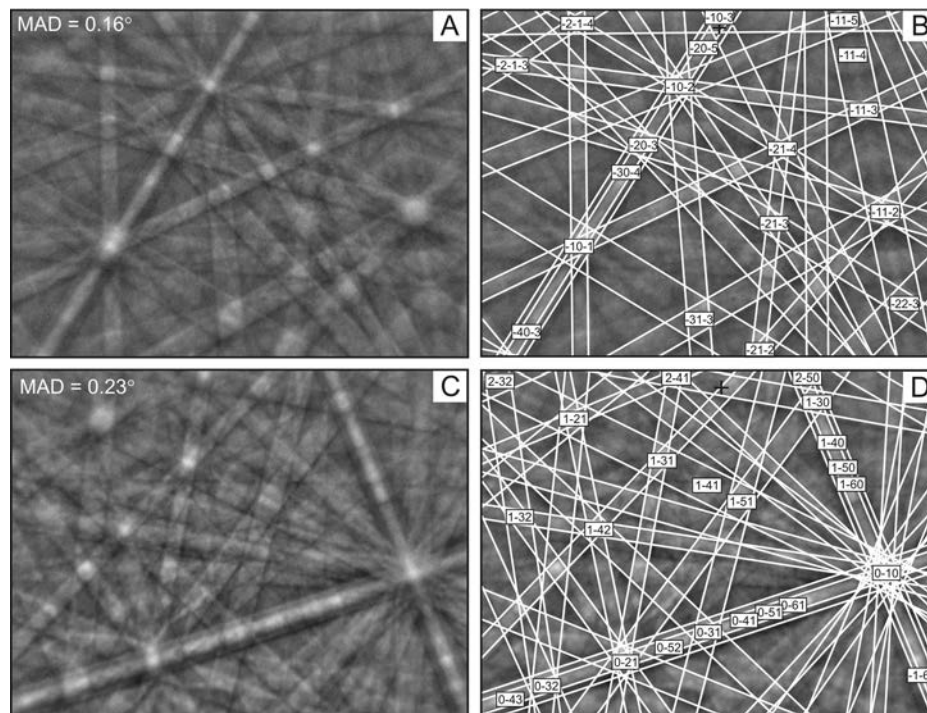


Fig. 2. EBSD patterns (A, C) and fitted result (B, D) obtained for crystals shown in Fig. 1D, point 7 (A, B) and in the inset on Fig. 1C, point 6 (C, D).

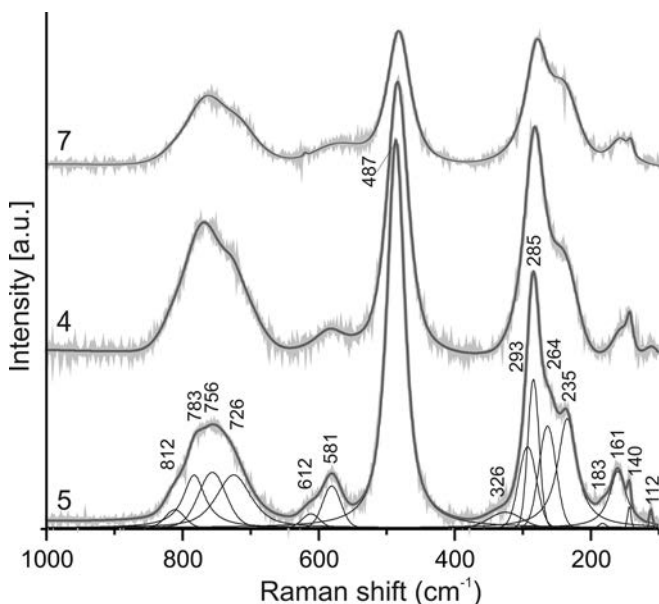


Fig. 3. Raman spectra of dzhuluite. Numbers correspond to the points of analyses in Table 1 and on Fig. 1.

appearance of a well-defined band at about  $600\text{ cm}^{-1}$  is rather a manifestation of asymmetric stretching vibrations in  $[\text{Fe}^{3+}\text{O}_4]^{5-}$  (Rulmont *et al.*, 1995).

The strong band at  $490\text{ cm}^{-1}$  due to bending vibrations in  $[\text{Fe}^{3+}\text{O}_4]^{5-}$  is characterized by a large half-width, attributed to the contribution to this vibration type of tetrahedra occupied by other cations. Bands near  $300\text{ cm}^{-1}$  are related to vibrations in  $[\text{R}(\text{ZO}_4)]$ , whereas bands below  $300\text{ cm}^{-1}$

are assigned to translation motions of  $T(\text{ZO}_4)$  and  $T(\text{Ca})$ . A characteristic feature of garnets of the bitikleite group with  $\text{Fe}^{3+}$  in tetrahedral site is a displacement of the bands at  $300$  and  $250\text{ cm}^{-1}$  towards lower frequencies in comparison with their Al-analogues (Galuskina *et al.*, 2010a). For example, on the bitikleite spectrum ( $\text{Al} > \text{Fe}$  at Z), these bands are at about  $303\text{ cm}^{-1}$  and  $252\text{ cm}^{-1}$  (Galuskina *et al.*, 2010a) and on the dzhuluite spectrum at  $285\text{ cm}^{-1}$  and  $235\text{ cm}^{-1}$ , respectively (Fig. 3).

Increasing uranium content leads to a decrease in the general intensity of the spectrum, especially for the bands related the bending vibrations at about  $490\text{ cm}^{-1}$ ; the spectrum is also blurred (Fig. 3). A similar effect was observed in the spectra of garnets of the elbrusite-kerimasite series (Galuskina *et al.*, 2010b).

## Discussion

Four Ca-garnet members, namely, bitikleite  $\{\text{Ca}_3[\text{Sb}^{5+}\text{Sn}^{4+}](\text{Al}^{3+}_3)\text{O}_{12}$ , usturite  $\{\text{Ca}_3[\text{Sb}^{5+}\text{Zr}^{4+}](\text{Fe}^{3+}_3)\text{O}_{12}$ , dzhuluite  $\{\text{Ca}_3[\text{Sb}^{5+}\text{Sn}^{4+}](\text{Fe}^{3+}_3)\text{O}_{12}$  and elbrusite  $\{\text{Ca}_3[\text{U}^{6+}_{0.5}\text{Zr}^{4+}_{1.5}](\text{Fe}^{3+}_3)\text{O}_{12}$  belong to the bitikleite group with the common crystal chemical formula  $\{\text{X}_3\}[\text{R}^{5+}\text{R}^{4+}](\text{R}^{3+}_3)\text{O}_{12}$  and double site occupation in the Y site (Galuskina *et al.*, 2010a–2010c; Grew *et al.*, 2013). The Nb-analogue of usturite  $\{\text{Ca}_3\}[\text{Nb}^{5+}\text{Zr}^{4+}](\text{Fe}^{3+}_3)\text{O}_{12}$  (Zaitsev *et al.*, 2011; Grew *et al.*, 2013), the Sn-analogue of elbrusite  $\{\text{Ca}_3\}[\text{U}^{6+}_{0.5}\text{Sn}^{4+}_{1.5}](\text{Fe}^{3+}_3)\text{O}_{12}$  (Galuskina *et al.*, 2010b; Grew *et al.*, 2013) and the Al-analogue of usturite  $\{\text{Ca}_3\}[\text{Sb}^{5+}\text{Zr}^{4+}](\text{Al}^{3+}_3)\text{O}_{12}$  (our

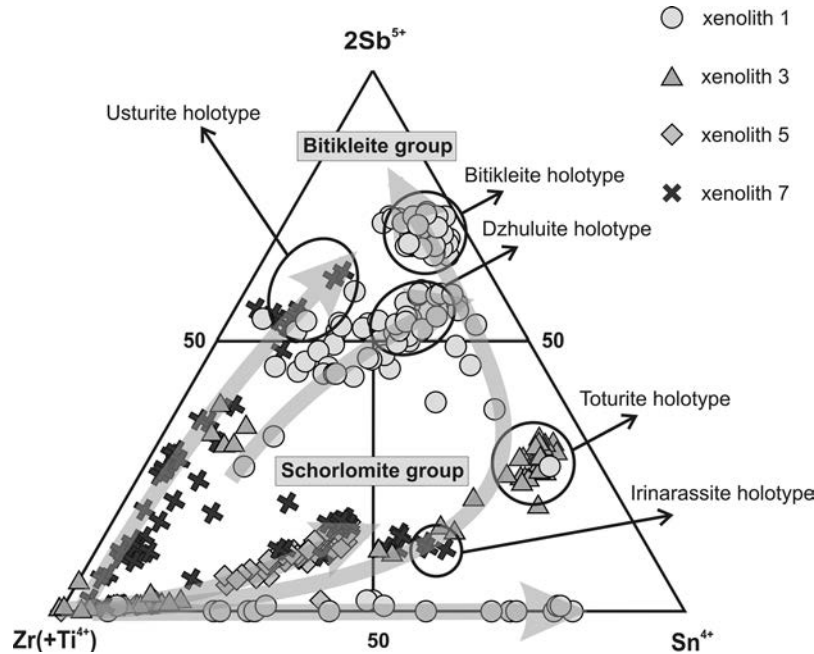


Fig. 4. Analytical points and compositional trends of minerals of the schorlomite and bitikleite groups from different xenoliths of the Upper Chegem Caldera.

unpublished data) are potential new mineral species of this group.

Dzhuluite is represented by the complex solid solution  $\text{Ca}_3[\text{Sb}^{5+}, \text{Sn}^{4+}, \text{Zr}, \text{U}^{6+}, \text{Ti}^{4+}]_2(\text{Fe}^{3+}, \text{Al}, \text{Fe}^{2+}, \text{Ti}^{4+}, \text{Si} \dots)_3\text{O}_{12}$ , which significantly complicates its classification in the context of the garnet supergroup nomenclature (Grew *et al.*, 2013). Even on the level of group crystal-chemical formulas, the problem arises. If we assign all tetravalent cations to the bitikleite  $\{\text{X}_3\}[\text{R}^{5+}\text{R}^{4+}](\text{R}^{3+}_3)\text{O}_{12}$  and schorlomite  $\{\text{X}_3\}[\text{R}^{4+}_2](\text{R}^{3+}_2\text{R}^{4+})\text{O}_{12}$  crystal-chemical formulas, a significant part of the uranium must be accommodated in the  $\{\text{Ca}_3\}[\text{U}^{6+}_2]\{\text{Fe}^{2+}_3\}\text{O}_{12}$  yafsonite end-member (Table 1). If, alternatively, all of the uranium is combined in the  $\{\text{Ca}_3\}[\text{U}^{6+}_{0.5}\text{Zr}_{1.5}](\text{Fe}^{3+}_3)\text{O}_{12}$  elbrusite end-member, the major part of the  $\text{Sb}^{5+}$  should be assigned to the  $\{\text{Ca}_3\}[\text{Sb}^{5+}_2](\text{Fe}^{3+}_2\text{Fe}^{2+})\text{O}_{12}$  end-member – unknown among natural garnets but corresponding to synthetic  $\text{Ca}_3\text{Sb}_2\text{ZnGa}_2\text{O}_{12}$  (Tolksdorf & Wolfmeier – Springer Materials - The Landolt-Börnstein Database). With this approach to its classification, the high-uranium analysis no. 8 in Table 1 will belong to elbrusite, with a  $\{\text{Ca}_3\}[\text{U}^{6+}_{0.5}\text{Zr}_{1.5}](\text{Fe}^{3+}_3)\text{O}_{12}$  end-member content of 57 mol%. In this case, calculation on the end-members (even by grouping some) cannot be attempted because more than three cations are simultaneously present at two sites [Y] and [Z] (Table 1). As was shown by Grew *et al.* (2013), classification of this type of garnet should be based on the charge at the Z site and the dominant-valence rule, taking double site occupation into consideration (Hatert & Burke, 2008). For the dzhuluite analyses, the charge at the Z site varies in the range 8.75–8.97 and the proportion of the Z site occupied by  $\text{Fe}^{3+}$ , defining the content of the dzhuluite

end-member, fluctuates between 58 and 68.5% (Table 1). At the Y site  $\text{Sb}^{5+}$  and Sn are the predominant cations (Table 1). The proportion of the  $\text{Sb}^{5+}$ ,  $\text{Sn}^{4+}$  pair in dzhuluite, which determines double site occupation at the Y site, is above 65% (Table 1). In summary, the ideal end-member of these garnet analyses will be represented by the crystal-chemical formula  $\{\text{Ca}_3\}[\text{Sb}^{5+}\text{Sn}^{4+}](\text{Fe}^{3+}_3)\text{O}_{12}$ .

The classification of the elbrusite that is associated with dzhuluite, and which is characterized by a high content of dzhuluite end-member, is still more complicated (Table 1, analysis 8). The charge at the Z site of 8.7 allows it to be classified in the bitikleite group (Grew *et al.*, 2013). The total occupancy at the Y site of  $\text{R}^{4+} = 0.866 \text{ apfu}$ ,  $\text{R}^{5+} = 0.466 \text{ apfu}$  and  $\text{R}^{6+} = 0.531 \text{ apfu}$  sums up to  $1.863 \text{ apfu}$  (Table 1), a content of di- and trivalent cations that is insignificant and that has no influence on the classification problems. The charge of approximately 9, characteristic for garnet in the bitikleite group, and the significant quantity of penta- and hexavalent cations point to double-site occupation at the Y site with marked predominance of the  $\{\text{X}_3\}[\text{R}^{6+}_{0.5}\text{R}^{4+}_{1.5}](\text{R}^{3+}_3)\text{O}_{12}$  end-member over  $\{\text{X}_3\}[\text{R}^{5+}\text{R}^{4+}](\text{R}^{3+}_3)\text{O}_{12}$  as  $\frac{1}{2}\text{R}^{5+} \text{ apfu} \ll \text{R}^{6+} \text{ apfu}$ . As the  $\text{U}^{6+}$  content is  $> 0.5 \text{ apfu}$ , it is necessary to consider that part of the uranium will be grouped in the  $\{\text{Ca}_3\}[\text{U}^{6+}_2]\{\text{Fe}^{2+}_3\}\text{O}_{12}$  yafsonite end-member (Table 1). In the composition of this garnet, an increased content of Ca is characteristic of partially metamict uranium-bearing garnet of the bitikleite group (Galuskina *et al.*, 2010a). The question of the valence of the uranium and iron is still open; to date, we have assumed all uranium to be hexavalent based on the fact that, in the case of all high-uranium garnets associated with vorlanite  $\text{CaU}^{6+}\text{O}_4$  for which U valence has been determined, it is so (Galuskina *et al.*, 2011). Nevertheless,



it is impossible to exclude the possibility that uranium in the garnet structure is stabilized in the pentavalent state. If so, then it would be related to the typical bitikleite end-member with the crystal-chemical formula  $\{X_3\}[U^{5+}R^{4+}](R^{3+}_3)O_{12}$ .

This study and previous investigations of garnet minerals from altered xenoliths of the Upper Chegem Caldera (Galuskina *et al.*, 2010a–c) reveal the sequence of high-temperature garnet crystallization (Fig. 4). Firstly, zirconian garnets of the schorlomite group (kerimasite, kimzeyite) form. This is followed by stannian garnets of the schorlomite group (toturite and irinarassite) and/or zirconian and stannian garnets of the bitikleite group (bitikleite, dzhuluite, usturite). Elbrusite usually crystallizes last. The latest garnets known from altered xenoliths in the Upper Chegem Caldera are represented by schorlomite, andradite, grossular, fluorine-bearing katoite and its  $Fe^{3+}$ -analogue which are, as a rule, developed near the contact with host ignimbrite.

**Acknowledgements:** We thank Pádraig Kennan for checking English of our manuscript. We express thanks to anonymous reviewers for their careful revisions and Christian Chopin for his assistance during preparation of this paper. I. G. is supported by the Ministry of Science and Higher Education of Poland, grant no. N307 09 7038.

## References

- Dodokin, A.P., Lyubutin, I.S., Mill, B.V., Peshkov, V.P. (1972): Mössbauer effect in antiferromagnetic substances with garnet structures. *J. Exp. Theor. Phys.*, **63**, 1002–1009 (in Russian).
- Galuskin, E.V., Gazeev, V.M., Armbruster, T., Zadov, A.E., Galuskina, I.O., Pertsev, N.N., Dzierzanowski, P., Kadiyski, M., Gurbanov, A.G., Wrzalik, R., Winiarski, A. (2008): Lakargiite  $CaZrO_3$ : A new mineral of the perovskite group from the North Caucasus, Kabardino-Balkaria, Russia. *Am. Mineral*, **93**, 1903–1910.
- Galuskin, E.V., Gazeev, V.M., Lazic, B., Armbruster, T., Galuskina, I.O., Zadov, A.E., Pertsev, N.N., Wrzalik, R., Dzierzanowski, P., Gurbanov, A.G., Bzowska, G. (2009): Chegemite  $Ca_7(SiO_4)_3(OH)_2$ —a new humite-group calcium mineral from the Northern Caucasus, Kabardino-Balkaria, Russia. *Eur. J. Mineral*, **21**, 1045–1059.
- Galuskin, E.V., Armbruster, T., Galuskina, I.O., Lazic, B., Winiarski, A., Gazeev, V.M., Dzierzanowski, P., Zadov, A.E., Pertsev, N.N., Wrzalik, R., Gurbanov, A.G., Janeczek, J. (2011): Vorlanite  $(CaU^{6+})O_4$  - A new mineral from the Upper Chegem caldera, Kabardino-Balkaria, Northern Caucasus, Russia. *Am. Mineral*, **96**, 188–196.
- Galuskin, E.V., Lazic, B., Armbruster, T., Galuskina, I.O., Pertsev, N.N., Gazeev, V.M., Włodyka, R., Dulski, M., Dzierzanowski, P., Zadov, A.E., Dubrovinsky, L.S. (2012): Edgrewite  $Ca_9(SiO_4)_4F_2$ -hydroxyedgrewite  $Ca_9(SiO_4)_4(OH)_2$ , a new series of calcium humite-group minerals from altered xenoliths in the ignimbrite of Upper Chegem caldera, Northern Caucasus, Kabardino-Balkaria, Russia. *Am. Mineral*, **97**, 1998–2006.
- Galuskina, I.O., Galuskin, E.V., Armbruster, T., Lazic, B., Dzierzanowski, P., Gazeev, V.M., Prusik, K., Pertsev, N.N., Winiarski, A., Zadov, A.E., Wrzalik, R., Gurbanov, A.G. (2010a): Bitikleite-(SnAl) and bitikleite-(ZrFe): New garnets from xenoliths of the Upper Chegem volcanic structure, Kabardino-Balkaria, Northern Caucasus, Russia. *Am. Mineral*, **95**, 959–967.
- Galuskina, I.O., Galuskin, E.V., Armbruster, T., Lazic, B., Kusz, J., Dzierzanowski, P., Gazeev, V.M., Pertsev, N.N., Prusik, K., Zadov, A.E., Winiarski, A., Wrzalik, R., Gurbanov, A.E. (2010b): Elbrusite-(Zr)—a new uranian garnet from the Upper Chegem caldera, Kabardino-Balkaria, Northern Caucasus, Russia. *Am. Mineral*, **95**, 1172–1181.
- Galuskina, I.O., Galuskin, E.V., Dzierzanowski, P., Gazeev, V.M., Prusik, K., Pertsev, N.N., Winiarski, A., Zadov, A.E., Wrzalik, R. (2010c): Toturite  $Ca_3Sn_2Fe_2SiO_{12}$ —A new mineral species of the garnet group. *Am. Mineral*, **95**, 1305–1311.
- Galuskina, I.O., Galuskin, E.V., Kusz, J., Dzierzanowski, P., Prusik, K., Gazeev, V.M., Pertsev, N.N., Dubrovinsky, L. (2011a): Bitikleite-(SnFe), IMA 2010–064. CNMNC Newsletter No. 8, April 2011, p. 290. *Mineral. Mag.*, **75**, 289–294.
- Galuskina, I.O., Galuskin, E.V., Prusik, K., Gazeev, V.M., Pertsev, N.N., Dzierzanowski, P. (2011b): Irinarassite, IMA 2010–073. CNMNC Newsletter No. 8, April 2011, p. 292. *Mineral. Mag.*, **75**, 289–294.
- Galuskina, I.O., Lazic, B., Armbruster, T., Galuskin, E.V., Gazeev, V.M., Zadov, A.E., Pertsev, N.N., Ježak, L., Wrzalik, R., Gurbanov, A.G. (2009): Kumtyubeite  $Ca_5(SiO_4)_2F_2$ —A new calcium mineral of the humite group from Northern Caucasus, Kabardino-Balkaria, Russia. *Am. Mineral*, **94**, 1361–1370.
- Galuskina, I.O., Lazic, B., Galuskin, E.V., Armbruster, T., Gazeev, V.M., Włodyka, R., Zadov, A.E., Dulski, M., Dzierzanowski, P. (2012): Fluorchegemite, IMA 2011–112. CNMNC Newsletter No. 13, June 2012, page 812. *Mineral. Mag.*, **76**, 807–817.
- Gazeev, V.M., Zadov, A.E., Gurbanov, A.G., Pertsev, N.N., Mokhov, A.V., Dokuchaev, A., Ya, N. (2006): Rare minerals of Verkhniy Chegem caldera (in skarned carbonates xenoliths in ignimbrites). *Vestnik Vladikavkazskogo Nauchnogo Centra*, **6**, 18–27 (in Russian).
- Grew, E.S., Locock, A.J., Mills, S.J., Galuskina, I.O., Galuskin, E.V., Hålenius, U. (2013): Nomenclature of the Garnet Supergroup. *Am. Mineral*, **98**, in press.
- Hatert, F., Burke, E.A.J. (2008): The IMA–CNMNC dominant-constituent rule revisited and extended. *Can. Mineral*, **46**, 717–728.
- Lazic, B., Armbruster, T., Savelyeva, V.B., Zadov, A.E., Pertsev, N.N., Dzierzanowski, P. (2011): Galuskinite,  $Ca_7(SiO_4)_3(CO_3)$ , a new skarn mineral from the Birkhin gabbro massif, Eastern Siberia, Russia. *Mineral. Mag.*, **75**, 2631–2648.
- Rulmont, A., Tarte, P., Van Moer, A., Cartié, B., Choynet, J. (1995): Simultaneous occurrence of  $Sn^{4+}$  on the three cationic sites of the garnet structure: the solid solutions  $Ca_xSn_xGa_{8-2x}O_{12}$  ( $2.5 < x < 3.0$ ). *J. Solid State Chem.*, **118**, 6–9.
- Shannon, R.D. (1976): Revised effective ionic radii and systematic studies of interatomic distances in halides and chalcogenides. *Acta Crystallogr A*, **32**, 751–767.
- Strocka, B., Holst, P., Tolksdorf, W. (1978): An empirical formula for the calculation of lattice constants of oxides garnets based on substituted yttrium- and gadolinium-iron garnets. *Philips J. Res.*, **33**, 186–202.



- Tolksdorf, W., Wolfmeier, U.: *Tables 67–88, Figs. 10–18*. Hellwege, K.-H., Hellwege, A. M. (ed.). SpringerMaterials - The Landolt-Börnstein Database (<http://www.springermaterials.com>). doi:10.1007/10201632\_6
- Williams, P.A., Hatert, F., Pasero, M., Mills, S. (2011): New minerals and nomenclature modifications approved in 2011. IMA Commission on New Minerals, Nomenclature and Classification (CNMNC), Newsletter 8. *Mineral. Mag.*, **75**, 289–294.
- Zaitsev, A.N., Williams, C.T., Britvin, S.N., Kuznetsova, I.V., Spratt, J., Petrov, S.V., Keller, J. (2011): Kerimasite,  $\text{Ca}_3\text{Zr}_2(\text{Fe}^{3+}_2\text{Si})\text{O}_{12}$ , a new garnet from carbonatites of Kerimasi volcano and surrounding explosion craters, Northern Tanzania. *Mineral. Mag.*, **74**, 803–820.

*Received 20 December 2012*

*Modified version received 18 January 2013*

*Accepted 12 February 2013*